Colloids and Surfaces B: Biointerfaces xxx (2015) xxx–xxx

Contents lists available at ScienceDirect

Colloids and Surfaces B: Biointerfaces

journal homepage: www.elsevier.com/locate/colsurfb

Characterization of the Interaction Between Pancreatic Trypsin and an Enteric Copolymer as a Tool for Several Biotechnological Applications

Mauricio Javier Braia, Dana Belén Loureiro, Gisela Tubio, Diana Romanini*

Instituto de Procesos Biotecnológicos y Químicos (IPROBYQ)-CONICET, Facultad de Ciencias Bioquímicas y Farmacéuticas, Universidad Nacional de Rosario, Rosario, Argentina

ARTICLE INFO

Article history:
Received 26 May 2015
Received in revised form 19 October 2015
Accepted 26 October 2015
Available online xxx

Keywords:
Trypsin
Polymer
Calorimetric techniques
Bioseparation
Immobilization

ABSTRACT

Protein-polyelectrolyte complexes are very interesting systems since they can be applied in many long-established and emerging areas of biotechnology. From nanotechnology to industrial processing, these complexes are used for many purposes: to build multilayer particles for biosensors; to entrap and deliver proteins for pharmaceutical applications; to isolate and immobilize proteins. The enteric copolymer poly(methacrylic acid-co-methyl methacrylate) 1:2 (MMA) has been designed for drug delivery although its chemical properties allow to use it for other applications. Understanding the interaction between trypsin and this polymer is very important in order to optimize the mechanism of formation of this complex for different biotechnological applications.The formation of the trypsin-MMA complex was studied by spectroscopy and isothermal titration calorimetry. Structural analysis of trypsin was carried out by catalytic activity assays, circular dichroism and differential scanning calorimetry. Isothermal titration calorimetry experiments showed that the insoluble complex contains 12 trypsin molecules per MMA molecule at pH 5 and they interact with high affinity to form insoluble complexes. Both electrostatic and hydrophobic forces are involved in the formation of the complex. The structure of trypsin is not affected by the presence of MMA, although it interacts with some domains of trypsin affecting its thermal denaturation as seen in the differential scanning calorimetry experiments. Its catalytic activity is not altered. Dynamic light scattering demonstrated the presence of a soluble trypsin-copolymer complex at pH 5 and 8. Turbidimetric assays show that the insoluble complex can be dissolved by low ionic strength and/or pH in order to obtain free native trypsin.

1. Introduction

Trypsin (TRP) is a protease widely used for numerous biotechnological and industrial processes [1]. TRP is a serin protease of 23.3 kDa with a high isoelectric point (11.4) and maximal catalytic activity at pH 8–8.2 [2]. It has 223 amino acids, 31 of them can present positive or negative charge according to the pH of the medium. They are 14 lysines (pKa=10.5), 2 arginines ($pK_a = 12.5$), 2 histidines ($pK_a = 6.0$), 2 aspartic acids ($pK_a = 3.9$) and 2 glutamic acids ($pK_a = 4.3$) [3]. At pH 5, the enzyme presents a theoretical net charge of $z = +7$ distributed on the surface of the molecule.

TRP is widely used in many industrial and pharmaceutical areas. Many studies were performed in our laboratory focusing on the interaction between TRP and polyvinyl sulfonic acid (PVS) and poly acrylic acid (PAA). However, these are non-biodegradable polymers and it is convenient to replace them with eco-friendly polymers, such as carrageenan, alginate or a wide variety of other methacrylates (Eudragits®).

The enteric copolymer poly(methacrylic acid-co-methyl methacrylate) 1:2 (MMA) is a biodegradable anionic copolymer with an average molecular mass of 125,000 [4]. This polymer might be soluble or insoluble depending on pH of the medium, temperature and the presence of certain ions and, therefore these kind of polymers are known as *smart or intelligent polymers* [5,6], *stimuli-responsive polymers* [7] or *environmental sensitive polymers* [8]. The interaction between proteins and these polymers is primarily by electrostatic forces to form complexes with various stoichiometry, structures and phase states. The biofunctionality of the proteins is not altered under most conditions, for this reason there has been a growing interest in the biotechnological applications of these complexes [9]. Systems containing protein-smart polymers complexes are very useful in several applications such as drug or

* Corresponding author at: Instituto de Procesos Biotecnológicos y Químicos (IPROBYQ)- CONICET, Facultad de Ciencias Bioquímicas y Farmacéuticas, Universidad Nacional de Rosario, Suipacha 531, (2000) Rosario, Argentina. Fax: +54 341 480 4598.
E-mail addresses: dromanini@conicet.gov.ar, dromani@fbioyf.unr.edu.ar (D. Romanini).

http://dx.doi.org/10.1016/j.colsurfb.2015.10.037
0927-7765/

protein delivery [10,11], bioseparation [12], immobilization [13], nanotechnology [14] and chromatography [15].

Globular proteins, such as TRP, and polyelectrolytes, such as MMA, can interact to form stable soluble or insoluble complexes. Many TRP molecules interact with one MMA molecule mainly through electrostatic forces and the formation of the complex highly depends on pH and ionic strength [16]. Although the TRP-MMA complex has been used to immobilize TRP from pancreas of mammalian, the complex was not completely characterized. In consequence, the recovery of the enzyme immobilization obtained was low [17].

The aims of this work were optimize the medium conditions that favor the interactions that allow the formation of the TRP-MMA insoluble complex and to analyze the conformational stability of TRP binding to MMA.

2. Material and methods

2.1. Chemical

Trypsin from porcine pancreas was purchased from Sigma Chem. Co. (USA) and the polymer MMA, was generously donated by Evonik Degussa Argentina S.A. Sodium citrate/TRIS–HCl and potassium phosphate buffer solutions of different pH were prepared at a concentration of 100 mM and 50 mM, respectively. The pH was adjusted with NaOH or HCl in each case. Stock solutions of 2.5% (w/w) MMA and 1 mM TRP pH 3.00 were prepared in appropriate buffer and the pH adjusted using HCl.

2.2. Phase diagrams of the TRP-MMA complex

To study the effect of the pH on the formation of the insoluble TRP-MMA complex at 25 °C, three solutions containing TRP and MMA were prepared at different TRP/MMA molar ratios (2.70; 5.34 and 13.35) with 100 mM citrate/TRIS–HCl buffer pH 3.00 and titrated with alkali and acid in order to cover the whole pH range. The absorbance at 420 nm (turbidity) was measured every 0.50 units of pH using a Jasco 520 spectrophotometer with a thermostatized cell of 1 cm of path length. Finally, turbidity was plotted vs. pH [18]. These phase diagrams show the pH range where the TRP-MMA complex is soluble or insoluble.

2.3. Circular dichroism (CD) of TRP in the presence of MMA

The CD spectra of TRP (0.25 mM) in the absence and presence of MMA (0.5% w/w) were performed in a Jasco spectropolarimeter, model J-815. The ellipticity values were obtained in mdeg directly from the instrument and 7 cycles were carried out to obtain the spectra. The samples were prepared with 50 mM phosphate buffer pH 5.00. The experimental error in spectral measurements is ±5%.

2.4. Enzymatic activity assay

TRP activity was determined with the substrate α-*N*-benzoyl DL-arginine-*p*-nitroaniline (BAPNA) using a method modified from Gildberg and Overbo [19]. BAPNA was prepared in 50 mM TRIS–HCl buffer pH 8.20 at a final concentration of 0.85 mM. The reaction is followed by measuring the absorbance at 400 nm of the released reaction product *p*-nitroanilide (molar absorptivity of 10,500 M^{-1} cm^{-1}) for 90 s. The absorbance of all solutions was measured using a Jasco 520 spectrophotometer. The activities were calculated from the slope of the absorbance 400 nm vs time straight lines. One unit of activity (U) was defined as the amount of enzyme required to release 1 μmol of *p*-nitroanilide per min.

In order to evaluate the enzyme stability at 25 °C in the presence of the MMA, TRP was incubated with different concentrations of MMA and the enzymatic activity was measured. The solutions were prepared with 100 mM citrate/TRIS buffer pH 5.00 and the concentration of TRP was the same for each molar ratio tested.

2.5. Isothermal titration calorimetry (ITC)

Measurements were performed at 25 °C by using a VP-ITC titration calorimeter (MicroCal Inc. USA). The sample cell was loaded with 1.436 mL of 0.3 mM TRP solution and the reference cell contained Milli-Q grade water. Titration was carried out using a 300 μL syringe, consecutively adding 5 μL aliquots of 0.175% (w/w) MMA solution to the cell containing the TRP solution. The experiments were performed in 50 mM citrate buffer pH 5.00, 50 mM citrate buffer pH 5.00 supplemented with 1.00 M NaCl and 50 mM TRIS–HCl buffer pH 8.00, respectively.

The resulting data set was fitted using MicroCal ORIGIN 7.0 software supplied with the instrument and the intrinsic molar enthalpy change for the binding (ΔH_b), the binding stoichiometry (n), and the intrinsic binding constant (k) were obtained. The equation for determining the heat associated to each injection is:

$$Q = \frac{nM_t \Delta H_b V_o}{2}\left(1 + \frac{1}{nkM_t} + \frac{X_t}{nM_t} - \sqrt{\left(1 + \frac{1}{nkM_t} + \frac{X_t}{nM_t}\right)^2 - \frac{4X_t}{nM_t}}\right) \quad (1)$$

where V_0 is the active volume cell, X_t is the bulk concentration of ligand and M_t is the bulk concentration of the macromolecule in V_0 [20].

The mathematical model equation selected to fit the ITC data was derived from a model that assumes the polyelectrolyte molecule binds to several protein molecules, all with the same affinity. In other words, the polyelectrolyte was considered as a macromolecule having *n independent and equivalent sites,* all of which have the same affinity constant, *K*, for the ligand (TRP) [21].

The heat associated to the MMA-TRP interaction (ΔH_b) was calculated using the Eq. (2):

$$\Delta H_b = \Delta H_t - \Delta H_d - \Delta H_{dissol} \quad (2)$$

where ΔH_t is the total heat associated to each MMA aliquot added to the TRP solution, ΔH_d is the heat of dilution of the MMA in buffer in the absence of TRP and ΔH_{dissol} is the heat of MMA dissolution. The heat associated to the dilution of TRP in buffer during the experiment was negligible. Then ΔH_b was plotted vs. MMA/TRP molar ratio and the affinity constant (K) and number of MMA molecules (n) bound per TRP molecule were calculated by non-linear fitting.

The intrinsic molar free energy change (ΔG°) and the intrinsic molar entropy change (ΔS°) for the binding reaction were calculated by the fundamental thermodynamic Eqs. (3) and (4):

$$\Delta G^\circ = -RT\ln K \quad (3)$$

$$\Delta S^\circ = \frac{\Delta H^\circ - \Delta G^\circ}{T} \quad (4)$$

2.6. Differential scanning calorimetry (DSC)

Thermal denaturation of TRP in the absence and presence of MMA was performed with a high sensitivity MicroCal Inc. differential scanning calorimeter (model VP-DSC) [22]. The solutions of 0.3 mM TRP were prepared in 50 mM citrate buffer pH 5.00 and 50 mM TRIS–HCl buffer pH 8.00; in the absence and presence of polymer (MMA/TRP molar ratio = 0.092). The scanning was performed in triplicate, between 25 and 85 °C at a scan rate of 30 °C h^{-1} and a constant pressure of 28 psi. Buffer baseline scans were determined by 10 repetitions and subtracted from TRP transition scans prior to normalization and analysis of the denaturation of TRP. Finally, the values of the excess heat capacity were obtained [23]. These calorimetric data were analysed using the software MicroCal

Please cite this article in press as: M.J. Braia, et al., Characterization of the Interaction Between Pancreatic Trypsin and an Enteric Copolymer as a Tool for Several Biotechnological Applications, Colloids Surf. B: Biointerfaces (2015), http://dx.doi.org/10.1016/j.colsurfb.2015.10.037

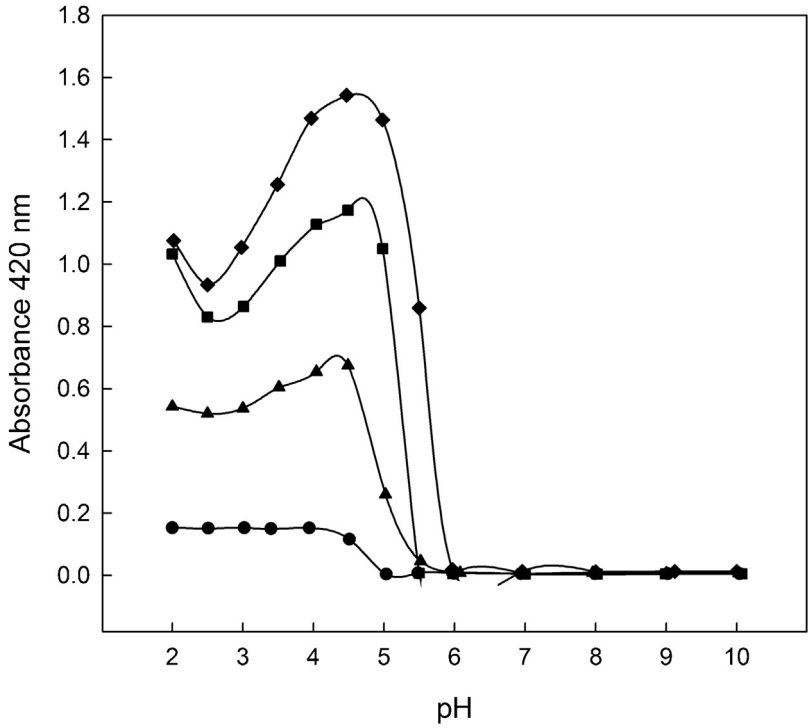

Fig. 1. Phase diagram of the TRP-MMA complex at different TRP/MMA molar ratios: (●) without TRP; (▲) 2.70; (■) 5.34 and (♦) 13.35. Medium 100 mM citrate/TRIS–HCl. Temperature 25 °C.

Inc. ORIGIN 7.0, according to the methodology recommended by IUPAC. The parameters obtained from this analysis were: the temperature at which maximum heat exchange occurs (T_m), the area under the peak, which represents the enthalpy of transition assuming that the process is reversible (ΔH_{cal}) and the vanít Hoff enthalpy (ΔH_{VH}). The evaluation of ΔH_{VH} gives an idea of the mechanism of the unfolding process of the TRP [24].

2.7. Dynamic light scattering (DLS)

The measurements were carried out using an ALV/CGS-3 equipped with a 22 mW He–Ne laser (632.8 nm) as light source; at scattering angle of 90° and a temperature of 25 °C. The viscosity and refractive index was 0.89222 cP and 1.332 for all systems, respectively. The matching liquid for the refractive index was cis-decalin.

Several experiments were carried out in 50 mM buffer citrate pH 5.00; 50 mM citrate buffer pH 5.00 supplemented with 1.00 M NaCl and 50 mM TRIS–HCl buffer pH 8.00. Solutions of TRP, MMA and mixtures of both were prepared in each buffer. The concentration of TRP and MMA were 0.1 mM and 30 μM, respectively. In the experiment performed with the mixture of both at pH 5.00, 100-fold lower concentrations where used in order to avoid the appearance of turbidity.

We used the homodyne intensity–intensity correlation function $G(q, t)$ where q, the amplitude of the scattering vector, is given by Eq. (5) [25]:

$$q = \frac{4\pi i \sin\left(\theta/2\right)}{\lambda} \tag{5}$$

For a Gaussian distribution of the intensity profile of the scattered light, $G(q, t)$ is related to the electric field correlation function $g(q, t)$ by Eq. (6) [26]:

$$G(q, \tau) = B\left(1 + \beta|g(q, \tau)|^2\right) \tag{6}$$

where B is the experimental baseline, β is a constant depending on the number of coherence areas generating the signal ($0 < \beta < 1$) and τ is the decaying time.

The statistical and mathematical analysis of the correlation function relates q and τ with the diffusion coefficient D through Eq. (7):

$$D = \frac{1}{q^2 \times \tau} \tag{7}$$

The hydrodynamic ratio R_h of each particle was calculated using the Einstein–Stoke equation (8) [27]:

$$D = \frac{k_b T}{6\pi\eta R_h} \tag{8}$$

The software GENDIST (GenR 94 v. 4.0) was used to perform the inverted Laplace transform using the REPES algorithm (*Regularized Positive Exponential Sum Program*) and to determine the R_h.

2.8. Data analysis

All experiments were performed in triplicate and all graphing and statistical analysis were carried out using the software SigmaPlot 10.0 for Windows (unless otherwise noted) which uses the Marquardt–Lavenberg algorithm [28].

3. Results and discussion

3.1. Phase diagrams of the TRP-MMA complex.

Fig. 1 shows the phase diagrams of the TRP-MMA complex. It can be seen that the formation of the TRP-MMA complex was highly influenced by the pH medium. At pH lower than 6.00, TRP and MMA molecules possess opposite charges and so, the insoluble complex between the two is formed. Between pH 5.00 and 6.00, turbidity is only due to the presence of the insoluble complex. Below pH 4.50, turbidity is due to the insoluble MMA and the insoluble complex.

Please cite this article in press as: M.J. Braia, et al., Characterization of the Interaction Between Pancreatic Trypsin and an Enteric Copolymer as a Tool for Several Biotechnological Applications, Colloids Surf. B: Biointerfaces (2015), http://dx.doi.org/10.1016/j.colsurfb.2015.10.037

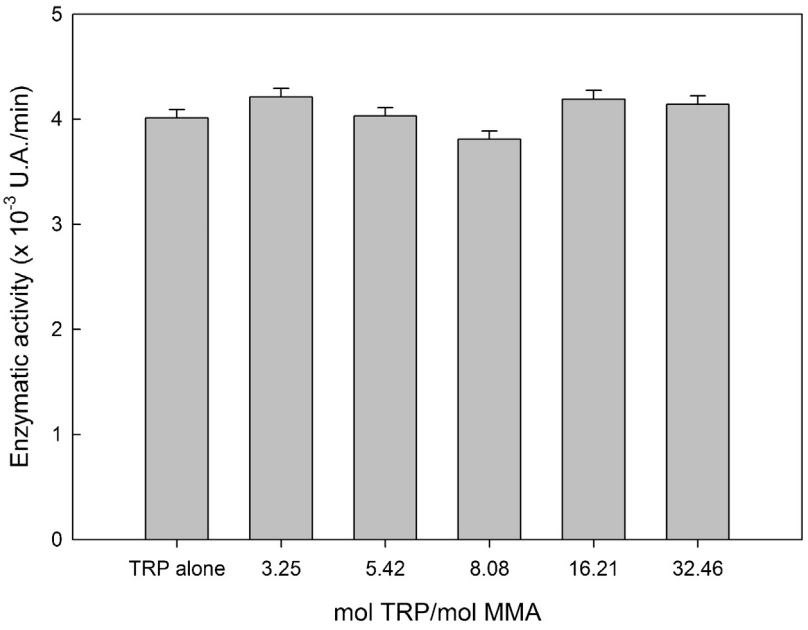

Fig. 2. Enzymatic activity of TRP at different TRP/MMA molar ratios. Medium 100 mM citrate/TRIS–HCl pH 5.00. Temperature 25 °C. Values are mean ± S.D. (n = 3).

The increase in the pH above 6.00 induced a large decrease in turbidity values, which suggests that no amount of insoluble complex is formed. The pH selected to perform the subsequent assays was 5.00 in order to obtain the insoluble TRP-MMA complex.

These experiments indicate that the maximum quantity of complex is formed at pHs 4–5.5 (TRP/MMA molar ratio around 13) and allowed us to design ITC experiments.

3.2. Circular dichroism of TRP in the presence of MMA

The secondary structure of a protein can be determined by CD measurement in the far UV (260–200 nm) region. The changes due to interaction of MMA with TRP on the secondary structure of the protein were followed by CD measurements at pH 5.00. The chromophores in this wavelength region are peptide backbone itself. The peptide backbone exhibits intense circular dichroism bands when it is located in regular, rigid confirmations of the protein backbone chain. In the far-UV region, the CD spectrum of TRP comprises of strong negative ellipticities at 208 and 222 nm. The negative ellipticity at 208 nm is more negative than that at 222 nm, indicating that TRP presents rich regions of α-helix and β-sheet [29].

The shape of the spectra of TRP obtained in the absence and presence of MMA was not modified in the presence of the polymer (data not shown). Also, the intensity of the peaks at 208 nm and 220 nm did not significantly change. These findings indicate that the secondary structure of the TRP is not altered when it is forming an insoluble complex with the MMA. Besides, it is necessary to evaluate the enzymatic capacity of the TRP in the presence of MMA.

3.3. Enzymatic activity of TRP in the presence of MMA

Fig. 2 shows a plot of enzymatic activity of TRP vs. TRP/MMA molar ratios. It can be seen that the enzymatic activity remains the same at each molar ratio tested (including the experiment performed in the absence of MMA). This indicates that the catalytic site of TRP is not altered by MMA.

Circular dichroism and enzymatic activity experiments have demonstrated that the secondary structure of TRP is not altered when it is forming a complex with MMA. In order to further analyse the effect of MMA in the structure enzyme, calorimetric techniques were used.

Table 1
Thermodynamic and binding parameters of the TRP-MMA interaction obtained by ITC. Values are mean ± S.D. (n = 3).

Parameters	Value
n (MMA mol/TRP mol)	$7.94.10^{-2} \pm 9.10^{-4}$
K (M^{-1})	$1.14.10^{6} \pm 4.10^{4}$
ΔH° (kcal/mol)	54.2 ± 0.5
ΔS° (e.u.)	210 ± 9
ΔG° (kcal/mol)	−8.31 ± 0.05

3.4. Isothermal titration calorimetry

Fig. 3 shows the binding-isotherm graph obtained plotting ΔH vs. MMA/TRP molar ratio. The experimental data was fitted to a *single set of identical sites* model. It was assumed that many TRP molecules binds to a single MMA molecule with the same affinity constant K. The parameters calculated are summarized in Table 1.

It can be seen that, on average, 12.57 TRP molecules were bound to one MMA molecule. The affinity constant showed a high value indicating that the interaction between the TRP and the MMA is very strong. The ΔH_b (normalized per mol of MMA injected) was positive, indicating that the interaction between the TRP and the MMA is an endothermic reaction and so, needs to absorb heat from the medium. Finally, the positive value of ΔS° indicates that the disorder of the system increases due to the release of structured water molecules.

ITC experiments performed in the presence of NaCl showed values of heat similar to those obtained when measuring the heat of dilution of the polymer. This result indicates that the TRP and the MMA are not interacting when NaCl concentration reaches 1.00 M in the buffer (data not shown) and suggests that electrostatic interactions play some role in the formation of the complex. Nevertheless, the positive values of ΔH° and ΔS° were consistent with the presence of hydrophobic interactions between TRP and MMA when both are forming an insoluble complex.

3.5. Differential scanning calorimetry

Figs. 4 and 5 show the thermal unfolding of TRP. It can be seen that both the shape and the integrated area of the melt-

Please cite this article in press as: M.J. Braia, et al., Characterization of the Interaction Between Pancreatic Trypsin and an Enteric Copolymer as a Tool for Several Biotechnological Applications, Colloids Surf. B: Biointerfaces (2015), http://dx.doi.org/10.1016/j.colsurfb.2015.10.037

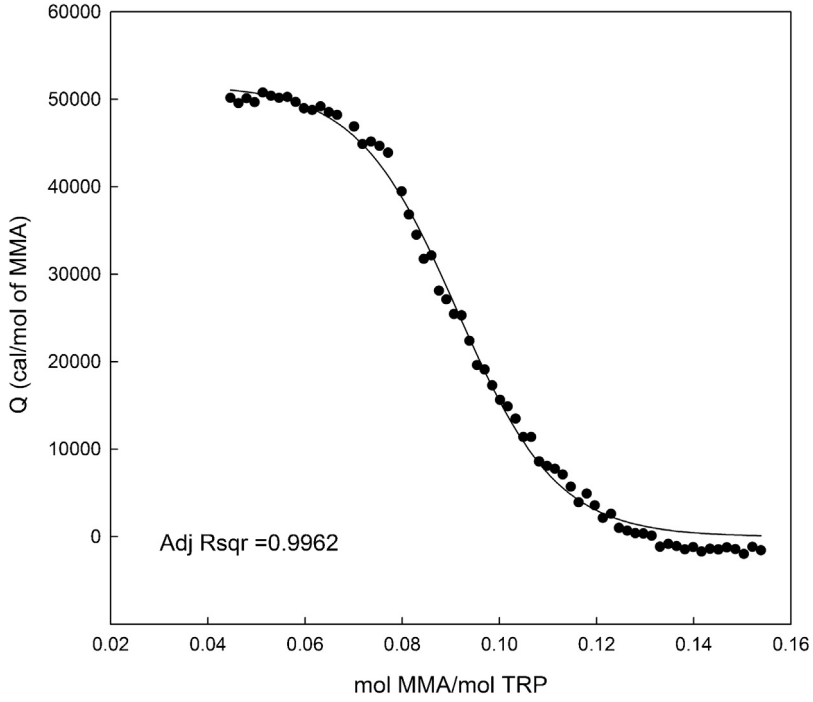

Fig. 3. Binding isotherm of the interaction between TRP and MMA. Model: single set of identical sites. Medium 100 mM citrate/TRIS–HCl pH 5.00. Temperature 25 °C.

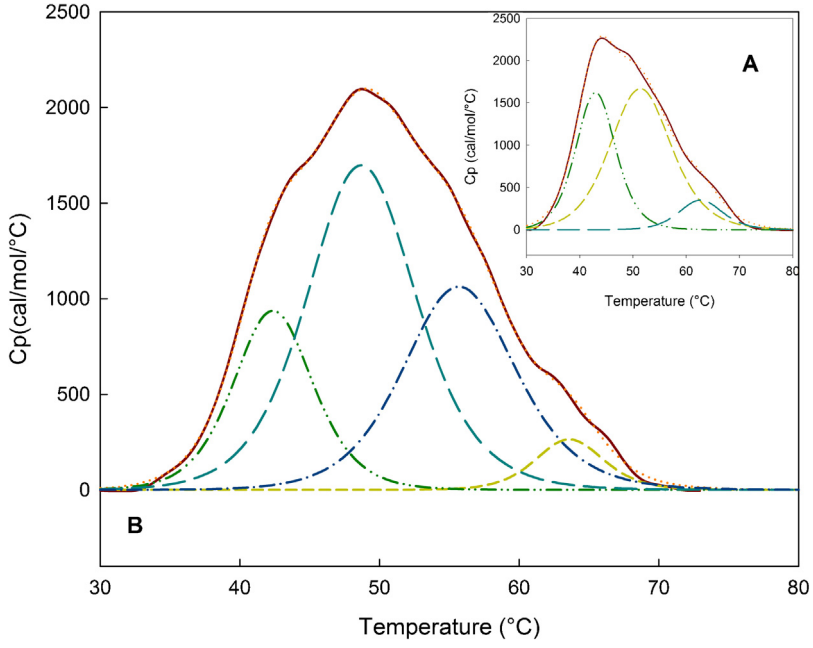

Fig. 4. Thermal unfolding of TRP in the (A) absence and (B) presence of MMA. Medium 100 mM citrate/TRIS–HCl pH 5.00.

Table 2
Denaturation parameters of TRP unfolding in the absent and presence of MMA.Values are mean ± S.D. (n = 10).

System	Transitions	T_m (°C)	ΔHcal(kcal/mol)	pH
TRP	1	51.6 ± 0.2	25.7 ± 2.5	5.00
	2	43.1 ± 0.1	16.2 ± 1.7	
	3	62.8 ± 0.4	3.8 ± 0.9	
TRP-MMA	1′	48.8 ± 0.1	17.6 ± 2.2	
	1″	55.7 ± 0.2	11.5 ± 1.7	
	2	42.4 ± 0.1	7.1 ± 0.8	
	3	63.6 ± 0.1	1.7 ± 0.3	
TRP	1	51.4 ± 0.1	13.2 ± 0.7	8.00
	2	43.5 ± 0.1	55.5 ± 0.8	
TRP-MMA	1	50.6 ± 0.3	65.2 ± 3.6	
	2	43.0 ± 0.2	40.5 ± 3.5	

Please cite this article in press as: M.J. Braia, et al., Characterization of the Interaction Between Pancreatic Trypsin and an Enteric Copolymer as a Tool for Several Biotechnological Applications, Colloids Surf. B: Biointerfaces (2015), http://dx.doi.org/10.1016/j.colsurfb.2015.10.037

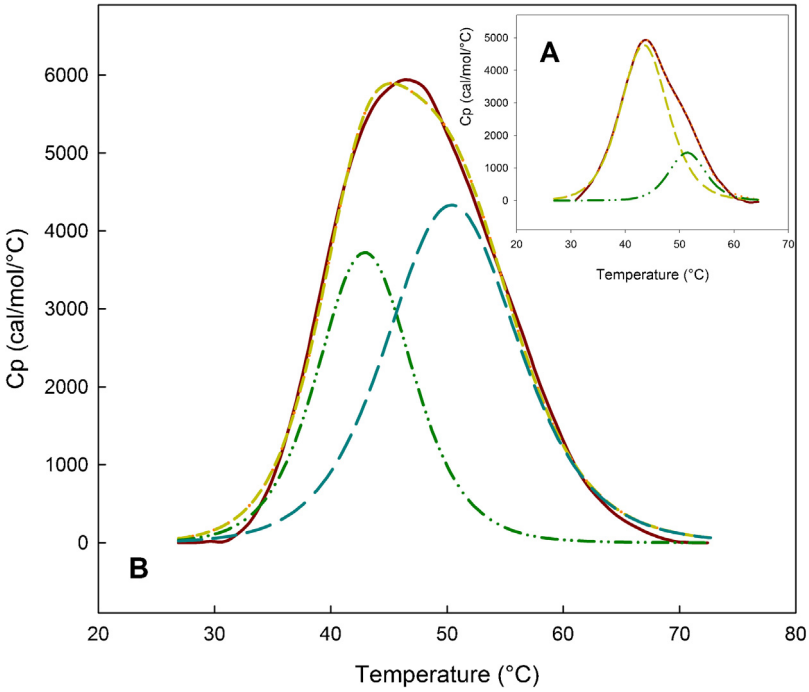

Fig. 5. Thermal unfolding of TRP in the (A) absence and (B) presence of MMA. Medium 100 mM citrate/TRIS–HCl pH 8.00.

ing curve were modified when the experiment was performe in buffer pH 5.00 (pH of complex formation) and pH 8.00 (pH maximal activity), in the absence and presence of MMA. The paran eters obtained by deconvolution of each curve are presented i Table 2.

It can be seen that TRP presented three transitions at pH 5.0 This indicates that the three domains independently unfold or from each other. In the presence of MMA, the first transition wa split into two transitions with smaller values of ΔH_{cal}, indicatin that MMA strongly interacts with this domain altering its mecha nism of unfolding. It is worth pointing out that the T_m of the ne transitions was 3 °C apart from the T_m of the first transition and th the sum of both ΔH_{cal} resulted in the ΔH_{cal} of the first transitior

The second and third transitions showed a decrease in the valu of ΔH_{cal} but no change in T_m. These findings suggest that MM also interacts with these domains but does not alter their therm stability.

At pH 8.00, TRP presented the first and second transitior observed at pH 5.00 with different ΔH_{cal}. In the presence of MM the ΔH_{cal} of the first transition was higher than in the absence MMA, while the ΔH_{cal} of the second transition was smaller. Thes results indicate that MMA interacts with both domains witho altering their thermal stability.

3.3. Dynamic light scattering

Fig. 6 shows the profile of R_h obtained for different systems. It can be seen that when the polyelectrolyte was incubated at pH 5.00, the particles presented an R_h of 252.9 nm. On the other hand, when pH was 8.00; two populations of particles with different R_h existed: 121.4 nm and 155.6 nm. TRP showed an R_h around 4.4 nm at both pH.

When TRP and MMA were incubated together at pH 5.00, the R_h measured was around 15 nm; much smaller than the R_h measured when the system only contains MMA at the same pH. This indicates that TRP and MMA interact at pH 5.00 to form a complex that is soluble due to the low concentrations of both the enzyme and the polyelectrolyte.

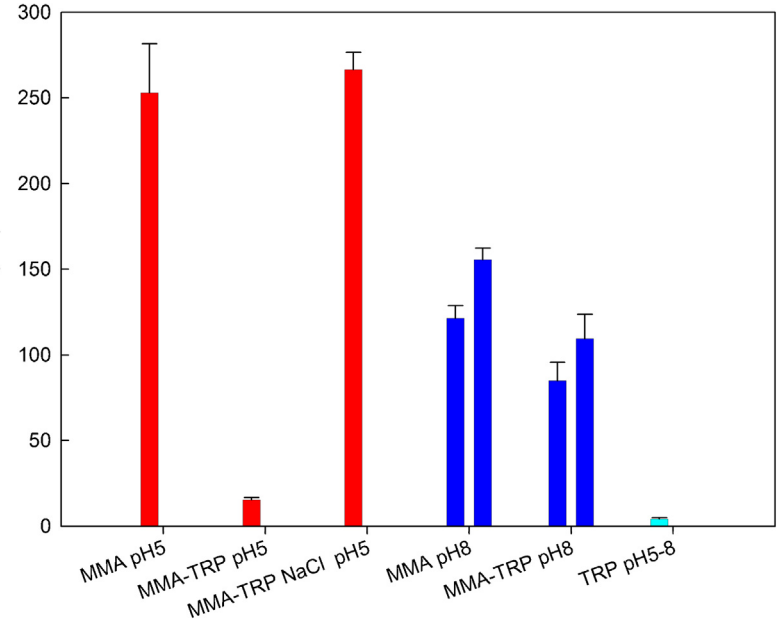

Fig. 6. Hydrodynamic ratio (R_h) of different systems: (■) MMA alone, MMA-TRP and MMA-TRP, 1.00 M NaCl, at pH 5.00; (■) MMA alone and MMA-TRP pH 8.00; (■) TRP pH 5.00 and 8.00. Medium 100 mM citrate/TRIS–HCl. Temperature 25 °C. Values are mean ± S.D. ($n = 3$).

When TRP and MMA were incubated together at pH 5.00, adding NaCl (1.00 M) to the medium, the R_h measured had the same value as the R_h measured in the system with MMA at pH 5.00. This indicates that the ionic strength inhibits the formation of the insoluble complex and corroborates the (partial) electrostatic nature of the interactions that drive the formation of the complex. These results agree with ITC experiments (Fig. 3).

Finally, a system prepared with TRP and MMA at pH 8.00 showed two populations of particles: one with R_h of 85 nm and the other with R_h of 120 nm. It can be seen that the R_h around 120–121 nm is

Please cite this article in press as: M.J. Braia, et al., Characterization of the Interaction Between Pancreatic Trypsin and an Enteric Copolymer as a Tool for Several Biotechnological Applications, Colloids Surf. B: Biointerfaces (2015), http://dx.doi.org/10.1016/j.colsurfb.2015.10.037

presented in the system TRP-MMA pH 8.00 as well as in the system MMA pH 8.00. On the other hand, both systems differed on the R_h of the second population: 85 nm in the presence of TRP and 155.6 nm in its absence. This difference indicates that TRP and MMA interact at pH 8.00 to form a complex. This complex is soluble since the solubility curves showed that a system prepared with TRP and MMA at pH 8.00 has no turbidity (Fig. 1).

4. Conclusions

Turbidimetric experiments indicate that the maximum quantity of complex is formed at pHs 4–5.5 when the TRP/MMA molar ratio is around 13. Similarly, ITC experiments at pH 5 demonstrate that 12.57 molecules of TRP bound to a molecule of MMA with high affinity. ITC results also demonstrate that the mechanism of interaction between TRP and MMA involves both hydrophobic and electrostatic interactions. However, according to the thermodynamic parameters, hydrophobic interactions are predominant.

DSC experiments show that MMA alters the mechanism of unfolding of TRP, however, the T_m is not modified enough to risk the thermodynamic stability of the enzyme. Furthermore, CD and enzymatic activity experiments indicate that the structure and catalytic capacity of TRP are not altered when it is forming a complex with MMA.

DLS experiments demonstrate the formation of a soluble TRP-MMA complex at pH 8.0. Also, DLS experiments performed at pH 5.0 showed that a soluble complex is formed prior to the formation of the insoluble complex. Each soluble complex is formed because of low charge density of TRP (at pH 8.0) and low TRP concentration, respectively.

Understanding the mechanism of formation of the TRP-MMA complex helps to optimize the biotechnological processes and/or technologies based on these complexes.

Founding sources

This work was supported by FonCyT No. PICT 2013-1730, BIO 391-UNR and CONICET PIP 551/2012.

Acknowledgements

We thank Dr. Watson Loh from the Institute of Chemistry at the University of Campinas (UNICAMP) for the use of the isothermal titration and the differential scanning calorimeters. We also thank Evonik Degussa Argentina S.A for donating the MMA (Eudragit® S100) and M. Robson, G. Raimundo, M. DeSanctis and M. Culasso for the language correction of the manuscript.

Appendix A. Supplementary data

Supplementary data associated with this article can be found, in the online version, at http://dx.doi.org/10.1016/j.colsurfb.2015.10.037.

References

[1] R. Beynon, J.S. Bond, Proteolytic Enzymes: A Practical Approach, 2nd ed., Oxford University Press, Oxford, 2001.
[2] T. Transue, J.M. Krahn, S.A. Gabel, E.F. De Rose, R.E. London, Biochem 43 (2004) 2829.
[3] A. Tziridis, D. Rauh, P. Neumann, P. Kolenko, A. Menzel, U. Brauer, C. Ursel, P. Steinmetzer, J. Sturzebecher, A. Schweinitz, T. Steinmetzer, M. Stubbs, Biol. Chem. 395 (2014) 891.
[4] J. Flora, B. Baker, D. Wybenga, Chemosphere 70 (2008) 1077.
[5] A. Hoffman, P.S. Stayton, V. Bulmus, G. Chen, C. Jinping, C. Chueng, J. Biomed. Mater. Res. 52 (2000) 577.
[6] I. Galaev, B. Mattiasson, Trends Biotechnol. 17 (2000) 335.
[7] B. Jeong, A. Gutowska, Trends Biotechnol. 20 (2002) 305.
[8] Y. Qiu, K. Park, Adv. Drug Deliv. Rev. 53 (2001) 321.
[9] A. Basak Kayitmazer, D. Seeman, B. Baykal Minsky, P. Dubin, Y. Xu, Soft Matter 9 (2013) 2553.
[10] H. James, R. John, A. Alex, K. Anoop, Acta Pharmacol. Sin. B 4 (2014) 120.
[11] S. Anandhakumar, V. Nagaraja, A.M. Raichur, Colloid Surf. B 78 (2010) 266.
[12] S. Wang, K. Chen, A.B. Kayitmazer, L. Li, X. Guo, Colloid Surf. B 107 (2013) 251.
[13] M. Sardar, I. Roy, M.N. Gupta, Enzyme Microb. Technol. 27 (2000) 672.
[14] K. Letchford, H. Burt, Eur. J. Pharm. Biopharm. 65 (2007) 259.
[15] J. Kobayashi, A. Kikuchi, K. Sakai, T. Okano, J. Chromatogr. A 958 (2002) 109.
[16] C.L. Cooper, P.L. Dubin, A.B. Kayitmazer, S. Turksen, Curr. Opin. Colloid Interface Sci. 10 (2005) 52.
[17] M. Sardar, R. Agarwal, A. Kumar, M.N. Gupta, Enzym. Microb. Technol. 20 (1997) 361.
[18] D. Takahashi, Y. Kubota, K. Kokai, T. Izumi, M. Hirata, E. Kokufuta, Langmuir 16 (2000) 3133.
[19] K. Atacan, M. Özacar, Colloid Surf. B 128 (2015) 227.
[20] W. Kim, Y. Yamasaki, K. Kataoka, J. Phys. Chem. B 110 (2006) 10919.
[21] N.S. Jha, N. Kishore, Thermochim. Acta 482 (2009) 21.
[22] A. Cooper, M.A. Nutley, A. Wadood, S.E. Harding, B.Z. Chowdhry, Protein-Ligand Interactions: Hydrodynamics and Calorimetry, 1st ed., Oxford University Press, Oxford, 2000.
[23] P.L. Privalov, Adv. Protein Chem. 33 (1979) 167.
[24] J.E. Ladbury, M.L. Doyle, Biocalorimetry: Applications of calorimetry the biological sciences, 1st ed., John Wiley & Sons, Ltd, Chichester, 2004.
[25] B.J. Berne, R. Pecora, Dynamic Light Scattering with Applications to Chemistry, Biology and Physics, 1st ed., Dover Publications Inc, Mineola, 2000.
[26] T. Nicolai, W. Brown, Scattering from concentrated polymer solutions, in: W. Brown (Ed.), Light Scattering: Principles and Development, Oxford University Press, Oxford, 1996, pp. 166–200.
[27] D. Some, S. Kenrick, Characterization of protein–protein interactions via static and dynamic light scattering, in: J. Cai, R.E. Wang (Eds.), Protein Interactions, InTech, Rijeka, 2012, pp. 401–426.
[28] D.W. Marquardt, J. Soc. Ind. Appl. Math. 11 (1963) 431.
[29] N.K. Prasanna Kumari, M.V. Jagannadham, Colloid Surf. B 82 (2011) 609–615.

Please cite this article in press as: M.J. Braia, et al., Characterization of the Interaction Between Pancreatic Trypsin and an Enteric Copolymer as a Tool for Several Biotechnological Applications, Colloids Surf. B: Biointerfaces (2015), http://dx.doi.org/10.1016/j.colsurfb.2015.10.037